

Learning Optical Flow for Fast MRI Reconstruction

Timothée Schmoderer

joint work with Noémie Debroux, Angelica I. Aviles-Rivero, Veronica Corona &
Carola-Bibiane Schönlieb

INSA Rouen Normandie

timothee.schmoderer@insa-rouen.fr

SIAM IS 2020 mini-symposium: The power of variational and hybrid multi-task models for image analysis.

July 17, 2020



- 1 Problem statement
- 2 Construction of the model
- 3 Algorithm description
- 4 Numerical experiments
- 5 Conclusions and Future works



T. Schmoderer, A. I Aviles-Rivero, V. Corona, N. Debroux and C-B. Schönlieb (2020)
Learning Optical Flow for Fast MRI Reconstruction
<https://arxiv.org/abs/2004.10464>.

Problem statement

MRI sampling issue: full acquisition takes a long time and produces motion blur \rightarrow undersampling.

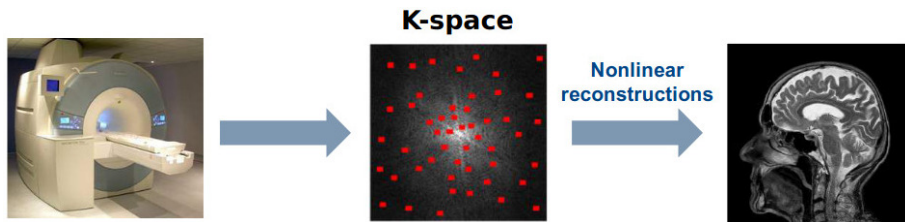


Figure: MRI acquisition process

Our problem: from a sequence of undersampled data:

$$\mathbf{f} : \Omega \times [0, T] \longrightarrow \text{undersampled k-space} \quad (1)$$

where the image domain Ω can be $2D$ or $3D$ spatial data, reconstruct faithful images of the body.

Basic Inverse Fourier Transform (ZF)

We now consider dynamic data. Let K be the undersampling Fourier operator:

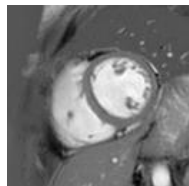
$$K : \Omega \longrightarrow \text{undersampled k-space} \quad (2)$$

it is seen as $K = \mathcal{U} \circ \mathcal{F}$ where \mathcal{F} is the usual Fourier transform and \mathcal{U} is an undersampling mask. We then consider the following least squares problem:

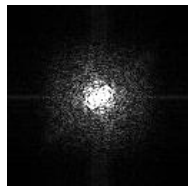
$$E(\mathbf{m}) = \int_0^T \frac{1}{2} \|K\mathbf{m}(t) - \mathbf{f}(t)\|_{L^2(\mathbb{R}^2)}^2 dt \quad (3)$$

where $\mathbf{m}(\mathbf{x}, t)$ is the reconstructed image sequence.

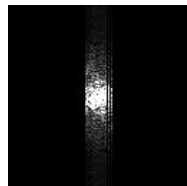
Basic Inverse Fourier Transform (ZF)



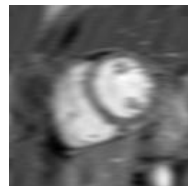
(a) Reference
Frame



(b) Fully sampled
k-space data



(c) Undersampled
k-space data: \mathbf{f}



(d) IFT
reconstruction:
 \mathbf{m}

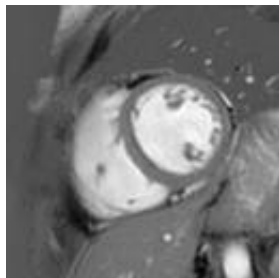
Figure: Inverse Fourier Transform Reconstruction

Compressed sensing (CS)

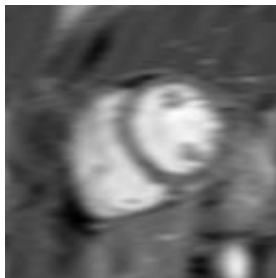
Compressed sensing for MRI, developed by [Lustig, 2007]. We add regularisation prior to improve the reconstruction quality.

$$E(\mathbf{m}) = \int_0^T \frac{1}{2} \|K\mathbf{m}(t) - \mathbf{f}(t)\|_{L^2(\mathbb{R}^2)}^2 + \lambda_1 TV(\mathbf{m}(t)) + \lambda_2 \|\Psi\mathbf{m}(t)\|_{L^1(\mathbb{R}^4)} dt$$

with TV regularisation (sharp edges), sparse wavelet representation.



(a) Reference Frame



(b) IFT Reconstruction

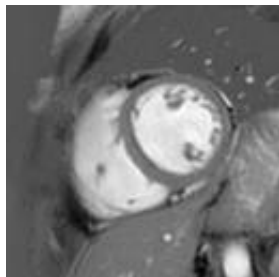


(c) CS Reconstruction

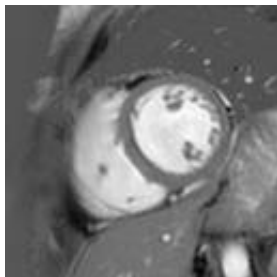
Figure: Compressed sensing Reconstruction (acceleration factor: 8)

Compressed Sensing and Motion Compensation

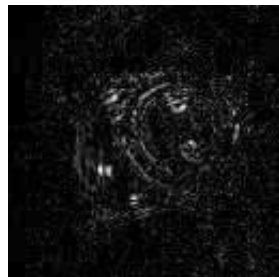
Idea: exploit the temporal correlation, corrupted by motion, between frames.



(a) Frame $t_0 = 0$



(b) Frame $t_1 = 1$



(c) $|t_1 - t_0|$

Figure: Temporal reference frames

We assume the **brightness constancy**, which after linearisation reads:

$$\frac{\partial \mathbf{m}}{\partial t} + \nabla \mathbf{m} \cdot \mathbf{u} = 0, \quad (4)$$

with $\frac{\partial \mathbf{m}}{\partial t}$ being the temporal derivative of the image sequence, $\nabla \mathbf{m}$ the spatial gradient, and $\mathbf{u} = [u_x, u_y]^T$ the unknown motion field.

To deal with the aperture problem, we embed the constraint in a variational formulation which reads:

$$\inf_{\mathbf{u}} E(\mathbf{u}) = \int_0^T \left\| \frac{\partial \mathbf{m}}{\partial t} + \mathbf{u} \cdot \nabla \mathbf{m} \right\|_{L^p(\Omega)}^p + \lambda \phi_r(\mathbf{u}) dt, \quad (5)$$

In the work of [Perez, 2013] authors proposed $p = 1$ and $\phi_r(\cdot) = TV(\cdot)$, which is known as the **TV-L¹ formulation**.

Compressed sensing with motion compensation (CS+M)

[Aviles-Rivero, 2018]

We joint the reconstruction and optical flow in one single model.

$$E(\mathbf{m}, \mathbf{u}) = \int_0^T \frac{1}{2} \|\mathbf{K}\mathbf{m}(t) - \mathbf{f}(t)\|_{L^2(\mathbb{R}^2)}^2 + \lambda_1 TV(\mathbf{m}(t)) + \lambda_2 \|\Psi\mathbf{m}(t)\|_{L^1(\mathbb{R}^4)} + \lambda_3 \left\| \frac{\partial \mathbf{m}}{\partial t} + \nabla \mathbf{m} \cdot \mathbf{u} \right\|_{L^1(\Omega)} + \lambda_4 TV(\mathbf{u}) dt \quad (6)$$

Drawback: poor quality of the optical flow, but still improve the reconstruction.

Dictionary learnt Optical Flow

Idea: Express the flow field as a sparse linear combination of basis functions in either off-the-shelf dictionaries or learnt ones.

$$\forall \mathbf{p} \in \mathcal{P}, R_{\mathbf{p}}\mathbf{u} = D\mathbf{a}_{\mathbf{p}}, \quad \text{with } \mathbf{a}_{\mathbf{p}} = ((a_x, a_y)_{\mathbf{p}})^T \text{ and } \|\mathbf{a}_{\mathbf{p}}\|_0 \text{ small.}$$

We consider,

- a discrete spatial setting,
- \mathcal{P} a partition of small overlapping patches of an optical flow,
- $R_{\mathbf{p}}$ the operator extracting patch \mathbf{p} ,
- a dictionary $D = \begin{bmatrix} D_x & 0 \\ 0 & D_y \end{bmatrix}$ where both D_x and D_y are composed of N_d elements such that $N_d \times |\mathcal{P}|$ is larger than the image dimension (\rightarrow over-complete dictionary).

Dictionary learnt Optical Flow



Figure: Scheme of the dictionary decomposition

This sparse representation over a learnt dictionary is incorporated in the variational setting through this term:

$$E_{\text{sparse}}(\mathbf{u}, \mathbf{a}) = \sum_{\mathbf{p} \in \mathcal{P}} \underbrace{\|R_{\mathbf{p}}\mathbf{u} - D\mathbf{a}_{\mathbf{p}}\|_F^2}_{\text{representation}} + \tau \underbrace{\|\mathbf{a}_{\mathbf{p}}\|_1}_{\text{sparsity}} \quad (7)$$

where $\|\cdot\|_F$ is the Frobenius norm and $\|\cdot\|_1$ is the l^1 norm.

Learning the dictionary

Given a reference optical flow \mathbf{u}^{ref} , the dictionary is learnt as the result of the following minimisation problem under constraints:

$$\begin{aligned} E(D, \mathbf{a}) &= \int_0^T \|\mathbf{R}_{\mathbf{p}}\mathbf{u}_{\mathbf{p}}^{ref} - D\mathbf{a}_{\mathbf{p}}\|_F^2 dt, & (8) \\ \|D_{x,j}\|_2 &\leq 1, \quad \|D_{y,j}\|_2 \leq 1, \quad 1 \leq j \leq N_d, \\ \|\mathbf{a}_{\mathbf{p}}\|_0 &\leq k_0 \quad \forall \mathbf{p} \in \mathcal{P}, \end{aligned}$$

where the pseudo norm $l^0(\cdot)$ counts the non-zero elements of $\mathbf{a}_{\mathbf{p}}$. The constraints on D ensure uniqueness of the solution

The discrete formulation of *our proposed joint and hybrid model* after the learning step of the dictionary reads:

$$\begin{aligned} \inf_{\mathbf{m}, \mathbf{u}, \mathbf{a}} E(\mathbf{m}, \mathbf{u}, \mathbf{a}) = & \int_0^T \frac{1}{2} \|\mathbf{K}\mathbf{m} - \mathbf{f}\|_F^2 + \lambda_1 TV(\mathbf{m}) + \lambda_2 \|\Psi\mathbf{m}\|_1 \quad (9) \\ & + \lambda_3 \left\| \frac{\partial \mathbf{m}}{\partial t} + \nabla \mathbf{m} \cdot \mathbf{u} \right\|_1 + \lambda_4 TV(\mathbf{u}) \\ & + \sum_{\mathbf{p} \in \mathcal{P}} \lambda_5 \|\mathbf{R}_{\mathbf{p}}\mathbf{u} - \mathbf{D}\mathbf{a}_{\mathbf{p}}\|_F^2 + \lambda_6 \|\mathbf{a}_{\mathbf{p}}\|_1 dt \end{aligned}$$

Recall: Chambolle & Pock iteration, proximal operators

We describe the Chambolle & Pock iteration as it is our elementary algorithmic brick. The Chambolle and Pock procedure aims at solving the nonlinear primal problem $\min_{x \in X} F(Cx) + G(x)$ with the following primal dual formulation:

$$\min_{x \in X} \max_{y \in Y} \langle Cx, y \rangle + G(x) - F^*(y). \quad (10)$$

Algorithm 1 Chambolle & Pock iteration [Chambolle, 2011]

Choose $\tau, \sigma > 0$ such that $\tau\sigma\|C\|^2 < 1$, $\theta \in [0, 1]$, $(x^0, y^0) \in X \times Y$ and set $\bar{x}^0 = x^0$

Update x^n, y^n and \bar{x}^n as follows:

$$\begin{cases} y^{n+1} &= (I + \sigma\partial F^*)^{-1}(y^n + \sigma C\bar{x}^n) \\ x^{n+1} &= (I + \tau\partial G)^{-1}(x^n - \tau C^*y^{n+1}) \\ \bar{x}^{n+1} &= x^{n+1} + \theta(x^{n+1} - x^n) \end{cases} \quad (11)$$

Recall: Chambolle & Pock iteration, proximal operators

where the proximal operators defined through (see [Combettes, 2011] for details):

$$x = (I + \tau \partial F)^{-1}(y) = \arg \min_x \left\{ \frac{\|x - y\|^2}{2\tau} + F(x) \right\}. \quad (13)$$

In the following we will describe only the closed form of the proximal operators.

Algorithm 2 MRIR-DLMC: Main Loop

Given a threshold $\epsilon > 0$.

Let \mathbf{m}^0 be a first approximation of the MRI sequence (ZF).

Let \mathbf{u}^0 be a first approximation of the optical flow ($TV - L^1$).

Learn the dictionary D (if needed).

Let \mathbf{a}^0 be a first approximation of the sparse decomposition of \mathbf{u}^0 in D (from the learning part).

repeat

 Compute $\mathbf{m}^{n+1} = \arg \min_{\mathbf{m}} E(\mathbf{m}, \mathbf{u}^n, \mathbf{a}^n)$

 Compute $\mathbf{u}^{n+1} = \arg \min_{\mathbf{u}} E(\mathbf{m}^{n+1}, \mathbf{u}, \mathbf{a}^n)$

 Compute $\mathbf{a}^{n+1} = \arg \min_{\mathbf{a}} E(\mathbf{m}^{n+1}, \mathbf{u}^{n+1}, \mathbf{a})$

until $\|\mathbf{m}^{n+1} - \mathbf{m}^n\| < \epsilon \|\mathbf{m}^n\|$

return \mathbf{m}^{n+1} .

Algorithm: Learn the dictionary

We fix a reference optical flow \mathbf{u}^{ref} and we optimise on D and \mathbf{a} .

Let $\bar{\mathbf{u}} = R\mathbf{u}^{ref} \in \mathbb{R}^{P_s^2 \times P_n \times (N_t-1)}$ be such that $\bar{\mathbf{u}}_k \in \mathbb{R}^{P_s^2 \times P_n}$ is the matrix of all patch extracted from $\bar{\mathbf{u}}$ at time k . The **joint optimisation** reads:

$$\min_{D \in \mathcal{D}, \mathbf{a} \in \mathcal{A}} E(D, \mathbf{a}) = \sum_{k=1}^{N_t-1} \frac{1}{2} \|\bar{\mathbf{u}}_k - D\mathbf{a}_k\|_F^2 \quad (14)$$

where the two convex constrained sets are given by,

$$\mathcal{D} = \{D : \|D_j\| \leq 1, \forall j\}, \quad \mathcal{A} = \{\mathbf{a} : \|\mathbf{a}\|_0 \leq k_0\}$$

Algorithm: Learn the dictionary

Finally,

$$D^{n+1} = \text{proj}_{\mathcal{D}} \left(D^n - \tau_1 \left(D^n \sum_{k=1}^{N_t-1} a_k a_k^T - \sum_{k=1}^{N_t-1} \bar{u}_k a_k^T \right) \right) \quad (15)$$

where the projection step is $\tau_1 < \frac{2}{\left\| \sum_{k=1}^{N_t-1} a_k a_k^T \right\|}$ and $\text{proj}_{\mathcal{D}}(D) = \frac{D}{\|D\|}$.

And:

$$a_k^{n+1} = \text{proj}_{\mathcal{A}} \left(a_k^n - \tau_2 D^T (D a_k^n - U_k) \right) \quad (16)$$

where this time, $\tau_2 < \frac{2}{\|DD^T\|}$. For $1 \leq j \leq P_n$ we denote $|\bar{a}_{k,j}(1)| \leq \dots \leq |\bar{a}_{k,j}(N_d)|$ the order of magnitude of the vector $a_{k,j} \in \mathbb{R}^{N_d}$. Then the projection operator on \mathcal{A} reads:

$$\forall 1 \leq i \leq N_d, \tilde{a}_{k,j}(i) = \begin{cases} a_{k,j}(i) & \text{if } |a_{k,j}(i)| \geq |\bar{a}_{k,j}(k_0)| \\ 0 & \text{otherwise.} \end{cases} \quad (17)$$

Minimise over the reconstructed image sequence \mathbf{m} :

$$E = \int_0^T \frac{1}{2} \|K\mathbf{m} - \mathbf{f}\|_2^2 + \lambda_1 \|\nabla\mathbf{m}\|_1 + \lambda_2 \|\Psi\mathbf{m}\|_1 + \lambda_3 \left\| \frac{\partial\mathbf{m}}{\partial t} + \nabla\mathbf{m} \cdot \mathbf{u} \right\|_1 dt$$

Let $C = [K, \nabla, \Psi, \partial_t + \mathbf{u} \cdot \nabla]^T$ be the operator acting on \mathbf{m} and $\mathbf{y} = [y_1, y_2, y_3, y_4]$ be the collection of dual variables.

With, the **Legendre-Fenchel conjugate** given by:

$$E^*(\mathbf{y}) = \int_0^T \frac{1}{2} \|y_1\|_2^2 + \langle y_1, f \rangle + \delta_{\{y: \|y\|_{2,\infty} \leq 1\}} \left(\frac{y_2}{\lambda_1} \right) + \delta_{\{y: \|y\|_\infty \leq 1\}} \left(\frac{y_3}{\lambda_2} \right) + \delta_{\{y: \|y\|_\infty \leq 1\}} \left(\frac{y_4}{\lambda_3} \right) dt$$

with the convex characteristic function $\delta_I(y) = 0$ if $y \in I$ and $+\infty$ otherwise.

The Chambolle-Pock [Chambolle, 2011] iteration then reads,

$$\begin{cases} \mathbf{y}^{n+1} &= (I + \sigma \partial E^*)^{-1}(\mathbf{y}^n + \sigma C \bar{\mathbf{m}}^n) \\ \mathbf{m}^{n+1} &= \mathbf{m}^n - \tau C^T \mathbf{y}^{n+1} \\ \bar{\mathbf{m}}^{n+1} &= \mathbf{m}^{n+1} + \theta(\mathbf{m}^{n+1} - \mathbf{m}^n) \end{cases} \quad (18)$$

And the proximal operator is given in closed form by:

$$(I + \sigma \partial E^*)^{-1}(\mathbf{y}) = \begin{cases} y_1 &= \frac{y_1 - \sigma f}{\sigma + 1} \\ y_2 &= \pi_{\lambda_1}(y_2) \\ y_3 &= \pi_{\lambda_2}(y_3) \\ y_4 &= \pi_{\lambda_3}(y_4) \end{cases}, \quad \pi_{\lambda}(y) = \frac{y}{\max\left(1, \frac{\|y\|_2}{\lambda}\right)} \quad (19)$$

π_{λ} : projection onto the unit ball.

Sparse representation

The minimisation over the variable \mathbf{a} can be split for each component \mathbf{a}_p which is given by $\tilde{E}(\mathbf{a}_p) = \lambda_5 \|R_p \mathbf{u} - D \mathbf{a}_p\|_F^2 + \lambda_6 \|\mathbf{a}_p\|_1$.

We take $F = \lambda_6 \|\cdot\|_1$, the proximal operator of its Legendre-Fenchel conjugate is given by the projection operator:

$$(I + \sigma \partial F^*)^{-1}(\mathbf{y}) = \pi_{\lambda_6}(\mathbf{y}) \quad (20)$$

Moreover since $G(\cdot) = \lambda_4 \|R_p \mathbf{u} - D \cdot\|_2^2$ is smooth, its resolvent reduces to the gradient,

$$\tau \nabla G(\mathbf{a}_p) = 2\tau \lambda_5 D^T (D \mathbf{a}_p - R_p \mathbf{u}). \quad (21)$$

Optical Flow approximation

Let $E(\mathbf{u}) = F(\nabla \mathbf{u}) + G(\mathbf{u})$ with $F(\cdot) = \lambda_4 \|\cdot\|_{2,1}$ and $G(\cdot) = \lambda_3 \left\| \frac{\partial \mathbf{m}}{\partial t} + \nabla \mathbf{m} \cdot \right\|_1 + \lambda_5 \sum_{\mathbf{p}} \|R_{\mathbf{p}} \cdot - D\mathbf{a}_{\mathbf{p}}\|_F^2$.

For simplicity of the notations we introduce the operators and notations:

$$\mathcal{A} = I + 2\tau\lambda_5 \sum R_{\mathbf{p}}^T R_{\mathbf{p}}, \quad \rho(\mathbf{u}) = \frac{\partial \mathbf{m}}{\partial t} + \mathbf{u} \cdot \nabla \mathbf{m}$$
$$\tilde{\mathbf{u}} = \mathbf{u} + 2\tau\lambda_5 \sum R_{\mathbf{p}}^T D\mathbf{a}$$

Then the proximal operator of G reads,

$$\mathcal{A}(I + \tau\partial G)^{-1}(\mathbf{u}) = \tilde{\mathbf{u}} + \begin{cases} -\lambda_3 \nabla \mathbf{m} & \text{if } \rho(\mathcal{A}^{-1}\tilde{\mathbf{u}}) > \tau\lambda_3 \mathcal{A}^{-1} \|\nabla \mathbf{m}\|^2 \\ \lambda_3 \nabla \mathbf{m} & \text{if } \rho(\mathcal{A}^{-1}\tilde{\mathbf{u}}) < -\tau\lambda_3 \mathcal{A}^{-1} \|\nabla \mathbf{m}\|^2 \\ -\rho(\tilde{\mathbf{u}}) \frac{\nabla \mathbf{m}}{\|\nabla \mathbf{m}\|^2} & \text{else} \end{cases}$$

and the F^* one is

$$(I + \sigma\partial F^*)^{-1}(\mathbf{y}) = \pi_{\lambda_6}(\mathbf{y}).$$

Framework

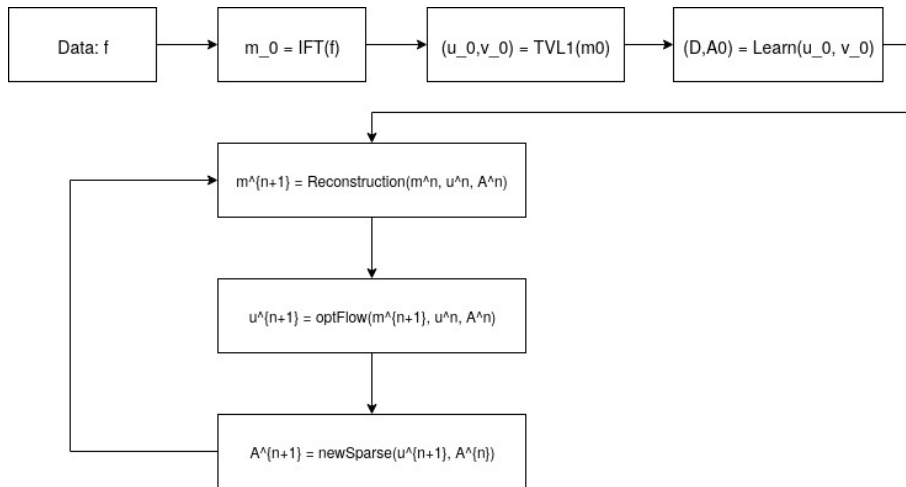


Figure: General workflow of the algorithm

We compare the quality of the results with the metrics:

$$SSIM(\mathbf{m}, \mathbf{m}_r) = \frac{(2\mu_{\mathbf{m}}\mu_{\mathbf{m}_r} + C_1)(2\sigma_{\mathbf{m},\mathbf{m}_r} + C_2)}{(\mu_{\mathbf{m}}^2 + \mu_{\mathbf{m}_r}^2 + C_1)(\sigma_{\mathbf{m}}^2 + \sigma_{\mathbf{m}_r}^2 + C_2)}$$

$$PSNR(\mathbf{m}, \mathbf{m}_r) = 10 \log_{10} \left(\frac{1}{\text{mean}((\mathbf{m}_r - \mathbf{m})^2)} \right)$$

We test against,

- ZF: pure IFT reconstruction,
- CS: compressed sensing [Lustig, 2007],
- LS: Low rank + sparsity (another state of the art method) [Otazo, 2013],
- CS+TVL1: compressed sensing and motion compensation [Aviles-Rivero, 2018],
- MC+JPDAL: recent improvement on CS+TVL1 [Zhao, 2019].

Parameters choice

Parameters chosen to optimise the metrics. Same parameters for all datasets

Main	Learning Dictionary	Reconstruction	Optical flow
$\lambda_1 = 3 \times 10^{-3}$	$D_n = 1024$	$\tau = 1/20$	$\tau = 1/25$
$\lambda_2 = 1 \times 10^{-4}$	$k_0 = 300$	$\sigma = 1/20$	$\sigma = 1/2$
$\lambda_3 = 1 \times 10^{-3}$		$\theta = 1$	$\theta = 1$
$\lambda_4 = 1 \times 10^{-3}$			
$\lambda_5 = 1 \times 10^{-3}$			
$\lambda_6 = 1 \times 10^{-4}$			
$\epsilon = 1 \times 10^{-4}$			

Table: Table of the Parameters

Datasets have size:

$$N_x = 128, N_y = 128 \text{ and } N_t \in \{14, 24, 30\}.$$

Presentation of the datasets

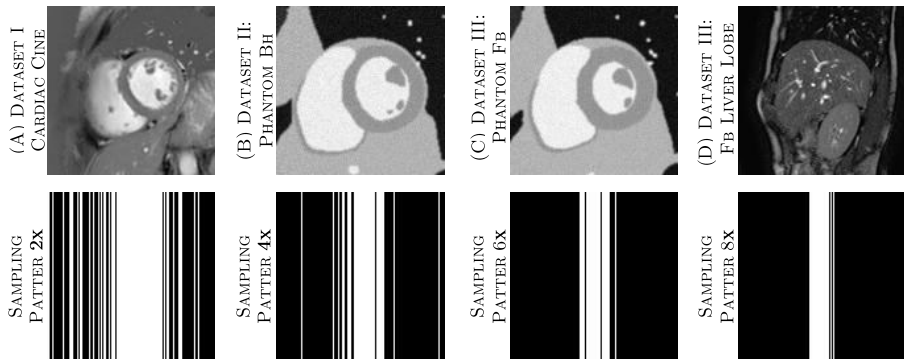
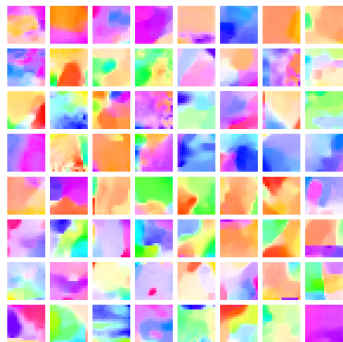
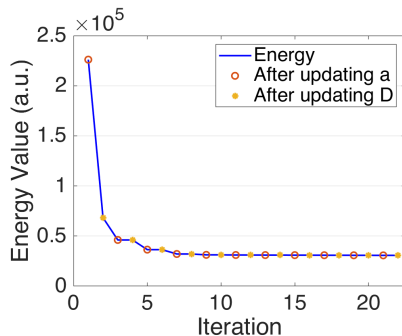


Figure: (Top column) Visual samples of the datasets used in our experiments. (Bottom column) visualisation of some undersampling patterns used in our experiments using acceleration factor = $\{2x, 4x, 6x, 8x\}$.

CINE Dictionary example



(A)



(B)

Figure: (A) Samples extracted from our learned dictionary with 1024 atoms and patches of size 16×16 . (B) Evolution of the energy during the learning process.

Results CINE and ETH

DATASET	RECONSTRUCTION SCHEME	2x		4x		6x		8x	
		PSNR	SSIM	PSNR	SSIM	PSNR	SSIM	PSNR	SSIM
Cardiac Cine	Zero-Filling	31.40	90.19	25.14	81.40	25	76.97	22.99	72.71
	CS	32.85	93.58	31.57	88.57	27.98	81.48	22.97	72.76
	L+S	34.21	92.77	31.09	86.20	27.74	80.10	22.98	72.68
	CS+M	36.72	96.23	31.53	90.26	28.39	80.17	24.9	72.68
	MC+JPDAL	36.7	97.85	32.72	92.06	27.80	84.29	23.15	75.51
	MRIR-DLMC	38.01	97.33	32.35	92.26	27.65	84.76	23.12	76.03
ETH	Zero-Filling	22.43	72.95	17.84	57.66	18.49	50.80	16.84	44.98
	CS	26.61	83.48	22.7	69.31	19.36	54.15	17.03	45.86
	L+S	24.26	77.68	21.71	63.39	19.19	52.46	16.82	44.96
	CS+M	31.91	91.73	25.86	76.32	21.14	58.37	20.01	49.17
	MC+JPDAL	32.81	93.07	27.3	82.01	22.34	65.62	19.39	54.1
	MRIR-DLMC	34.21	94.16	28.28	84.26	22.65	67.17	19.57	55.02

Table: Numerical comparison of our technique vs single and joint technique for different acceleration factors. The results are reported as the average of the corresponding metric over all the corresponding dataset.

Results Phantom FB and BH

DATASET	RECONSTRUCTION SCHEME	2x		4x		6x		8x	
		PSNR	SSIM	PSNR	SSIM	PSNR	SSIM	PSNR	SSIM
PHANTOM Free Breathing	Zero-Filling	28.27	78.87	23.97	68.08	20.53	61.39	22.57	61.09
	CS	31.91	83.11	28.58	76.35	24.83	67.01	22.58	61.12
	L+S	30.59	82.17	27.74	73.7	24.63	65.35	22.58	60.91
	CS+M	32.65	87.1	30.5	81.91	24.84	70.30	21.94	63.06
	MC+JPDAL	36.5	93	32.45	86.44	28.08	76.92	24.46	69.45
	MRIR-DLMC	33.19	88.46	30.5	82.77	27.76	76.18	25.14	71.9
PHANTOM Breath Holding	Zero-Filling	28.84	79.3	24.31	67.84	20.57	60.48	22.46	59.61
	CS	31.19	82.51	28.66	74.89	25.26	65.87	22.48	59.61
	L+S	30.59	82.8	27.99	72.93	24.9	64.5	22.46	59.38
	CS+M	32.11	86.13	30.02	89.16	24.28	67.74	21.55	60.59
	MC+JPDAL	35.37	91.86	31.24	83.85	27.3	74.16	24.14	66.66
	MRIR-DLMC	32.76	87.48	29.41	80.12	26.9	73.43	24.05	66.5

Transfer learning experiment

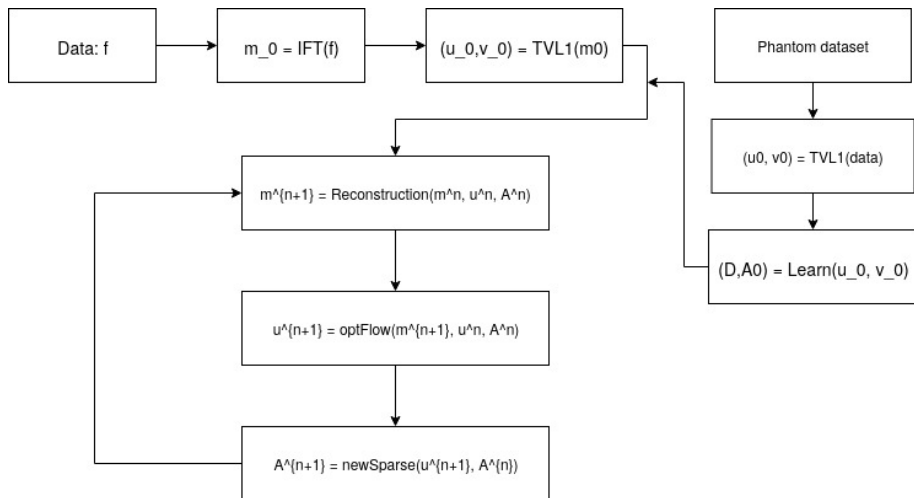


Figure: Experiment with outer dictionary

Transfer learning experiment results

DATASET	RECONSTRUCTION SCHEME	2x		4x		6x		8x	
		PSNR	SSIM	PSNR	SSIM	PSNR	SSIM	PSNR	SSIM
CARDIAC CINE	Zero-Filling	31.40	90.19	25.14	81.40	25	76.97	22.99	72.71
	CS	32.85	93.58	31.57	88.57	27.98	81.48	22.97	72.76
	L+S	34.21	92.77	31.09	86.20	27.74	80.10	22.98	72.68
	CS+M	36.72	96.23	31.53	90.26	28.39	80.17	24.9	72.68
	MC+JPDAL	36.7	97.85	32.72	92.06	27.80	84.29	23.15	75.51
	MRIR-DLMC	38.01	97.33	32.35	92.26	27.65	84.76	23.12	76.03
	MRIR-DLMC w/TL	37	97.05	31.79	90.71	27.70	84.85	24.80	81.01

Table: Numerical comparison of our technique vs other reconstruction methods. The numerical values are computed as the averages of the similarity metrics over the complete corresponding dataset. w/TL denotes the transfer learning capability of our technique, that is- the results are from training our dictionary with phantom datasets and applied to the real cardiac cine.

Conclusions and Future works

- **Novel mathematical model** to improve the reconstruction quality in dynamic MRI,
- **Single functional** embedding the reconstruction and the optical flow estimation,
- Motion estimation based on **dictionary learning**,
- **Efficient** and **tractable** optimisation framework,
- **Various** numerical experiments show the potential of our model,

Future works:

- Remove brightness constancy assumption,
- Study the effect of the size of the dictionary,
- Embed the proposed algorithm in a coarse to fine pyramidal approach.

Thank You!

References - 1



T. Schmoderer, A. I Aviles-Rivero, V. Corona, N. Debroux and C-B. Schönlieb (2020)

Learning Optical Flow for Fast MRI Reconstruction

<https://arxiv.org/abs/2004.10464>.



Lustig, Michael and Donoho, David and Pauly, John M (2007)

Sparse MRI: The application of compressed sensing for rapid MR imaging

Magnetic Resonance in Medicine: An Official Journal of the International Society for Magnetic Resonance in Medicine 58(6), 1182–1195.



Angelica I. Avilés-Rivero, Guy Williams, Martin J. Graves and Carola-Bibiane Schoenlieb (2018)

Compressed Sensing Plus Motion (CS+M): A New Perspective for Improving Undersampled MR Image Reconstruction

<http://arxiv.org/abs/1810.10828>.



Burger, Martin, Dirks, Hendrik and Schonlieb, Carola-Bibiane (2018)

A variational model for joint motion estimation and image reconstruction

SIAM Journal on Imaging Sciences 11(1), 94–128.

 Jia, Kui, Wang, Xiaogang and Tang, Xiaoou (2011)

Optical flow estimation using learned sparse model

2011 International Conference on Computer Vision 2391–2398.

 Chambolle, Antonin and Pock, Thomas (2011)

A first-order primal-dual algorithm for convex problems with applications to imaging

Journal of mathematical imaging and vision 40(1) 120–145.

 Combettes, Patrick L and Pesquet, Jean-Christophe (2011)

Proximal splitting methods in signal processing

Fixed-point algorithms for inverse problems in science and engineering 185–212.



Otazo, Ricardo and Emmanuel, C and Sodickson, Daniel K (2013)

Low-rank & sparse matrix decomposition for accelerated DCE-MRI with background & contrast separation

Proceedings of the ISMRM Workshop on Data Sampling and Image Reconstruction.



N. Zhao and D. O'Connor and A. Basarab and D. Ruan and K. Sheng (2019)

Motion Compensated Dynamic MRI Reconstruction with Local Affine Optical Flow Estimation

IEEE Transactions on Biomedical Engineering.